SAND2019-0201C

MCS11 *Tenerife, Spain, 16-20 June 2019*

MODELING THE DECOMPOSITION BEHAVIOR OF CARBON FIBER EPOXY COMPOSITE

SN Scott[1], AJ Kurzawski[1], VE Brunini[1], JC Hewson[1], JP Hidalgo[2], RM Hadden[3], S Welch[3]

snscott@sandia.gov

[1] Sandia National Laboratories

[2] University of Queensland

[3] University of Edinburgh

Abstract

Carbon fiber epoxy composites are increasingly used in systems requiring a material that is both strong and light weight, as in airplanes, cars, and pressure vessels. In fire environments carbon fiber epoxy composites are a fuel source subject to pyrolysis and oxidation. This study addresses modeling the thermal response of a carbon fiber composite material through heating and pyrolysis. Using TGA data, a decomposition mechanism is proposed to describe the decomposition and smoldering. This is then combined with a finite element conduction-radiation model with a porous media model for gas advection. Mass loss results are compared to cone calorimeter experiments where the composite was exposed to heat fluxes from 30 kW/m^2 to 80 kW/m^2. Two backing materials are compared, aluminum (a heat sink) and ceramic (an insulator). In the experiments, flaming ignition was observed. A heat flux is added to the surface of the composite to represent the heat generate by the flame, as gas phase combustion is not directly modeled. The agreement between the simulation and experiment are best for higher heat fluxes with the ceramic backing material due to the temperatures experienced by the composite in those cases.

Keywords: fire and explosions, carbon fiber epoxy composite, smoldering, pyrolysis

Introduction

Carbon fiber epoxy composites are an attractive engineering material due to their weight to strength ratio. Due to this, they have been extensively used in automotive and aeronautical industries, as well as other industries where a light weight, yet strong, material is advantageous. However, unlike more traditional engineering materials like metals, carbon fiber epoxy composites can be a source of fuel in a fire. At temperatures as low as 250C, epoxies can start to pyrolyze, creating flammable gasses. In order to understand the safety risks associated with these materials, it is necessary to understand their behavior in fire scenarios.

Many others have studied the burning behavior of carbon fiber epoxy composites. Quintiere *et al* explored the behavior of aircraft carbon fiber composites, finding a minim heat flux for the ignition of the material (18 kW/m^2) and creating a decomposition mechanism for the material [1]. Others have also created mechanisms for these types of composites as well as created thermo-physical properties [2]–[6]. Reviews of the interaction between structural modeling and fire behavior have been also been conducted [7]. Higher fidelity models have also been created using FireFOAM [8] and FEM codes to understand the implications of the fire on the structure [9].

Hidalgo *et al* investigated the behavior of composite material under fire like conditions in order to understand the safety risks associated with using these materials in pressure vessels [10]–[12]. A range of heat fluxes, thicknesses, and backing materials were examined using a cone calorimeter. Mass loss and temperature data were collected.

While experiments investigating the behavior of these materials are invaluable, the cost of burning complex systems made from expensive materials can be prohibitive. Validated high fidelity computational models can help fill this gap. They can allow for a range of designs and conditions to be tested to better understand the safety risks. To that end, this paper presents a numerical model for the pyrolysis and smoldering behavior of a carbon fiber epoxy composite. The model uses a porous media plus Arrhenius rate based chemistry modeling technique to describe the decomposition, heat transfer, and flow of a carbon fiber epoxy composite when exposed to a heat source. The model is compared to a subset of the experimental data collected by Hidalgo *et al* [10]–[12] to validate the numerical model. Specifically, the mass loss from 4.5mm thick samples exposed to heat fluxes ranging from 30kW/m^2 to 80kW/m^2 with two backing materials – one an insulator and one a heat sink.

Computational Model

The pyrolysis and smolder of the carbon fiber is computationally modeled using Sierra Thermal/Fluids: Aria, a multiphysics finite element code created at Sandia National Laboratories [13]. The composite is modeled as a porous media, which assumes that there are two phases, the condensed phase and the gas phase. The carbon fiber composite has a certain porosity, which is a function of reaction. In the gas phase, Darcy's law is used to approximate the flow of the fluid and the continuity, species, and enthalpy equations are solved. Gases are allowed to enter and exit the domain at specified boundaries. In the continuity equation, density is related to pressure through the ideal gas law so that the gas pressure can be solved. In the condensed phase the species and enthalpy equations are solved, and the two phases are coupled through source terms in the species equations and a volumetric heat transfer term in the enthalpy equations. This derivation is based on the model in Lautenberger *et. al.* [14]

The solid phase continuity equation is:

$$\frac{\partial \rho_b}{\partial t} = -\dot{\omega}'''_{fk} \tag{1}$$

where ρ_b is the bulk density, and $\dot{\omega}'''_{fk}$ is the formation rate of gas phase mass for the k^{th} species from the solid phase.

The porous gas phase continuity equation is:

$$\frac{\partial(\bar{\psi}\rho_g)}{\partial t} + \frac{\partial(\rho_g u_{j,g})}{\partial x_j} = \dot{\omega}'''_{fk} \tag{2}$$

where $\bar{\psi}$ is the mixture averaged condensed phase porosity, ρ_g is the gas density, and $u_{j,g}$ is the velocity of the gas using the Darcy approximation:

$$\bar{\psi} v_{j,g} = u_{j,g} = -\frac{\bar{K}}{\mu_g}\left(\frac{\partial p_g}{\partial x_j} + \rho_g g_j\right) \tag{3}$$

where $\bar{K}$ is the mixture averaged solid phase permeability tensor, μ_g is the gas phase viscosity and g_j is the gravity vector. The ideal gas law is used to relate the pressure to the density

$$\rho_g = \frac{\bar{M} p_g}{R T_g} \tag{4}$$

where $\bar{M}$ is the mass averaged molecular weight, R is the gas constant, and T_g is the gas temperature. The final porous gas phase continuity equation is then:

$$\frac{\partial}{\partial t}\left(\frac{\bar{M}p_g\bar{\psi}}{RT_g}\right)+\frac{\partial}{\partial x_j}\left(\frac{\bar{M}p_g}{RT_g}\frac{\bar{K}}{\mu_g}\left(\frac{\partial \rho_g}{\partial x_j}+\frac{\bar{M}p_g}{RT_g}g_j\right)\right)=\dot{\omega}'''_{fk} \tag{5}$$

The condensed phase species equation is:

$$\frac{\partial(\rho_b Y_k)}{\partial t}=\dot{\omega}'''_{fk}-\dot{\omega}'''_{dk} \tag{6}$$

where $\dot{\omega}'''_{fk}-\dot{\omega}'''_{dk}$ is the difference between the formation and destruction rates of gas phase mass for the k^{th} species and Y_k is the condensed phase mass fraction of the k^{th} species.

The gas phase species is:

$$\frac{\partial(\bar{\psi}\rho_g Y_{k.g})}{\partial t}+\frac{\partial(\rho_g u_{j,g} Y_{k.g})}{\partial x_j}=-\frac{\partial q^{Y,g}_{k,j}}{\partial x_j}+\left(\dot{\omega}'''_{s,fk}-\dot{\omega}'''_{s,dk}\right)+\left(\dot{\omega}'''_{g,fk}-\dot{\omega}'''_{g,dk}\right) \tag{7}$$

where $Y_{k.g}$ is the gas phase mass fraction of the k^{th} species, $\left(\dot{\omega}'''_{s,fk}-\dot{\omega}'''_{s,dk}\right)$ is the difference between the formation and destruction rates for heterogeneous reactions and $\left(\dot{\omega}'''_{g,fk}-\dot{\omega}'''_{g,dk}\right)$ is for homogenous reactions. $q^{Y,g}_{k,j}$ is the gas phase species diffusion flux, defined as:

$$q^{Y,g}_{k,j}=-\bar{\psi}\rho_g D_{k.g}\frac{\partial Y_{k.g}}{\partial x_j} \tag{8}$$

where $D_{k.g}$ is the gas phase mass diffusivity for the k^{th} species.

The gas phase enthalpy is:

$$\frac{\partial(\bar{\psi}\rho_g h_g)}{\partial t}+\frac{\partial(\rho_g u_{j,g} h_g)}{\partial x_j} = -\frac{\partial q^{h,g}_{k,j}}{\partial x_j}+\frac{\partial(\bar{\psi}p_g)}{\partial t}+h_{cv}(\bar{T}-T_g)+\sum_k\left(\dot{\omega}'''_{s,fk}-\dot{\omega}'''_{s,dk}\right)h_{k.g} \tag{9}$$

where h_g is the mixture averaged gas phase enthalpy, h_{cv} is the volumetric heat transfer coefficient, $\bar{T}$ is the porous condensed phase temperature, $h_{k.g}$ is the gas phase enthalpy of the k^{th} species. $q^{h,g}_j$ is the gas phase energy diffusive flux and is modeled as:

$$q^{h,g}_j=-\bar{\psi}\rho_g D_g\frac{\partial h_g}{\partial x_j} \tag{10}$$

where D_g is the mixture averaged gas phase mass diffusivity.

The condensed phase enthalpy is defined as:

$$\frac{\partial(\bar{\rho}c_p\bar{T})}{\partial t} = -\frac{\partial q_j^h}{\partial x_j} + h_{cv}(T_g - \bar{T}) \quad 11$$

where q_j^h is the condensed phase energy diffusive flux and c_p is the specific heat in the condensed phase:

$$q_j^{h,g} = -(k + k_e)\frac{\partial \bar{T}}{\partial x_j} \quad 12$$

Where k is the thermal conductivity and k_e is the effective conductivity for radiant heat transfer in optically thick media.

The domain of the simulation is designed to be a 2D representation of the experiment. In the experiment, the nominal size of the sample was 100mm x 100mm x 4.5mm and two materials were used on the back side of the carbon fiber epoxy composite: aluminum (a heat sink) and ceramic (an insulator). Mass loss data was collected for each backing material and for fluxes ranging from 30kW/m^2 to 80kW/m^2 (in increments of 10kW/m^2). A schematic is shown in Figure 1. For the numerical simulation, a structured mesh with an element edge length of 0.45mm was employed. The heat flux was applied the top surface of the carbon fiber. A convective boundary condition with a heat transfer coefficient of 5 and a far field temperature of 26C (300K) was applied to all surfaces. Also applied to all surfaces was a radiative boundary condition, also with a far field temperature of 26C (300K).

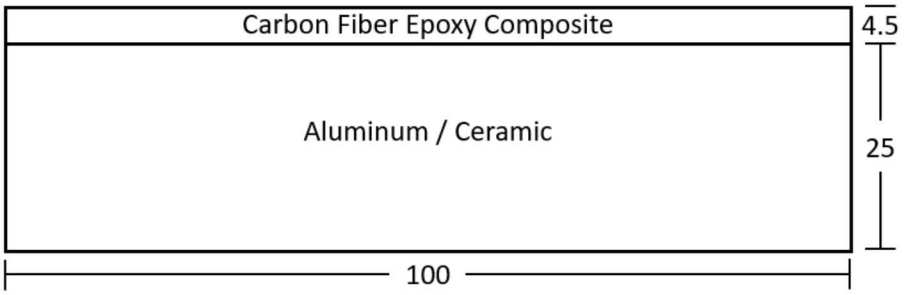

Figure 1. Schematic of the experiment. Dimensions are in mm.

The material properties used for the backing material are listed in Table 1. At the time of the experiments, material properties were not measured for the backing material, so literature values were used [15], [16]. However, the properties were measured for the carbon fiber epoxy composite and are presented in Table 2 along with properties used in the simulations. The simulation properties are defined the constituents of the carbon fiber epoxy composite and are volume averaged in order to take into account the changes in the material properties due to decomposition. Initially, the carbon fiber is 70% of the composite, and the epoxy 30%. All other constituents are 0%.

Table 1. Nominal Material Properties for backing material. The temperature range for the aluminum conductivity is 300K to 854K, for aluminum specific heat it is 200K to 600K

Parameter	**Value / Correlation**		**Units**
	Aluminum	*Ceramic*	
Conductivity	$-.0004\,\mathrm{T}^2 + 0.4711T + 52.8$	0.7	W/(mK)
Density	2700	1200	kg/m^3
Specific Heat	$0.5039\,\mathrm{T} + 745.72$	800	J/(kg/k)
Emissivity	0.1	0.5	-

Table 2. Nominal Material Properties for the composite. The simulation properties are defined the constituents of the carbon fiber epoxy composite and are volume averaged. The temperature range for the carbon fiber conductivity and specific heat for the simulation is 300K to 2328K.

Parameter	**Value / Correlation**		**Units**
	Simulation	*Experiment*	
Conductivity		$0.405\ (\mathrm{T}/293.15)^{0.8}$	W/(mK)
Epoxy	0.145		
Carbon Fiber	$0.335\ln(T) - 1.8257$		
CharA	0.029		
CharB	0.029		
Residue	0.00725		
Density		1360	kg/m^3
Epoxy	408		
Carbon Fiber	952		
CharA	650		
CharB	650		
Residue	2000		
Specific Heat		$4.1\,\mathrm{T} + 880\ [20 \le T \le 100]$ $10\,\mathrm{T} + 290\ [100 \le T \le 120]$ $1.85\,\mathrm{T} + 1270\ [120 \le T \le 180]$	J/(kg/K)
Epoxy	866		
Carbon Fiber	$4.0997\,\mathrm{T} - 369.12$		
CharA	936		
CharB	936		
Residue	866		
Permeability		-	m^2
Epoxy	2.42e-15		
Carbon Fiber	2.42e-14		
CharA	2.83e-12		
CharB	2.83e-12		
Residue	2.42e-11		
Emissivity	0.91	0.91	-

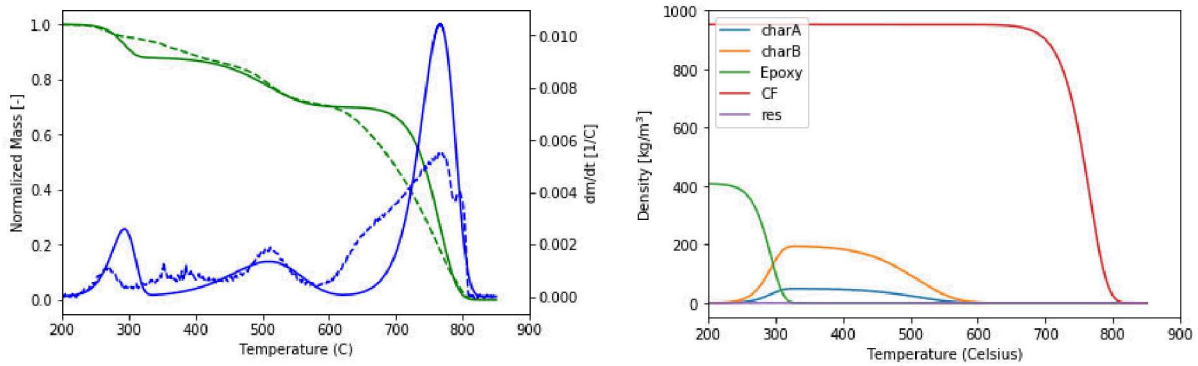

(a) (b)

Figure 2. (a) Comparison of simplified mechanism (solid) to TGA (dashed) for normalized mass loss (green) and the derivative of normalized mass loss (blue). (b) Depletion of solid phase species for simplified decomposition mechanism

As part of the experimental program, thermogravimetric analysis (TGA) was conducted [10]. Figure 2(a) shows the mass loss for oxidative conditions at a heating rate of 5 C/min. Figure 2(b) shows the density change (i.e. change in mass) for each constituent of the simulation. Along with the experimental TGA in Figure 2, is the mass loss curve given by the simplified mechanism proposed in equation 13 using the information from [2], [12]. Table 3 gives the kinetic parameters for the proposed mechanism.

$$
\begin{aligned}
&(1) \quad Epoxy \rightarrow CharA + fuel \\
&(2) \quad Epoxy \rightarrow CharB + fuel \\
&(3) \quad CharA \rightarrow Residue + gas \\
&(4) \quad CharB \rightarrow Residue + gas \\
&(5) \quad Carbon\ Fiber + O_2 \rightarrow Residue + gas
\end{aligned}
\qquad 13
$$

Table 3. Kinetic parameters. A is pre-exponential factor, E_a is the activation energy, ν is the stoichiometric coefficient of the solid phase product (on a mass basis), and H is the heat release.

	A	**E_a**	**ν**	**H**
	[1/s]	*[J/kmol]*	*mass based*	*[kJ/kg]*
Reaction 1	3.33 e11	1.47 e8	0.5	0
Reaction 2	1.325 e11	1.47 e8	0.5	0
Reaction 3	1895	9.15 e7	.0001	12730
Reaction 4	1895	9.15 e7	.0001	12730
Reaction 5	9.475 e14	3.48 e8	.0001	24770

Comparison of Simulations to Experiments

Figure 3 compares the simulations to the experimental results. The quality of the agreement between the experiments and the simulation vary with the heat flux and backing material. Generally, higher heat fluxes with the ceramic material have the best agreement. Qualitatively, the trends seen in the experiments are repeated in the simulation: the initial slope of the mass loss is lower for the aluminum backed material than for the ceramic. Additionally, the flattening of the mass loss curve seen in the ceramic backing experiments is replicated, whereas a more gradual mass loss is seen in the aluminum backed samples.

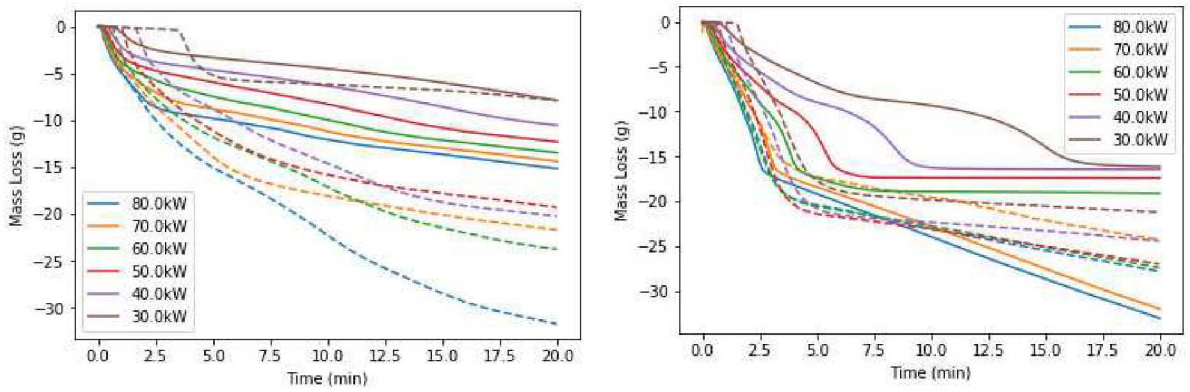

(a) (b)

Figure 3. Comparison of simulations (solid) to experiments (dashed) for heat fluxes from 30kW to 80kW for (a) the aluminum back face and (b) the ceramic back face

In order to understand divergences from the experiments, the density (i.e. change in mass) of the constituent species was examined. Figure 4 and Figure 5 show the change in density for the 80kW and 30kW experiments, for the aluminum and ceramic backing, respectively.

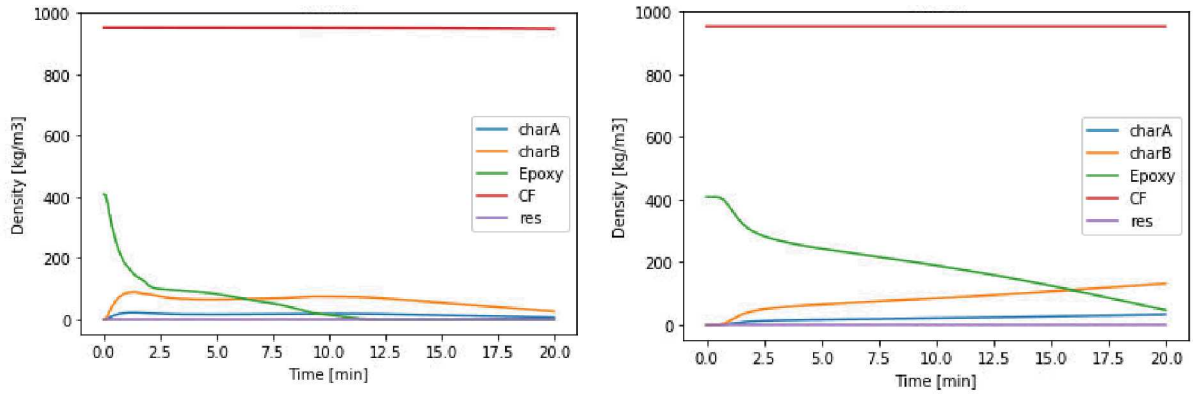

(a) (b)

Figure 4. Depletion of solid phase species for the simulation for the aluminum back faces for (a) 80kW flux and (b) 30kW flux

For the aluminum backed samples, the mass loss of epoxy is much slower than in the ceramic samples. In addition, the chars are not fully consumed, and the carbon fiber reaction is not activated. This accounts for the lower mass loss seen than in the corresponding experiments. In addition, the 30kW ceramic experiment has a flattening between 7 and 16 minutes not seen in the experiments. This is due to the char relations not progressing. In general, the ceramic 80kW sample has the best agreement: the fast initial mass loss generated by the epoxy and char reactions, followed by a slow mass loss governed by the carbon fiber reaction.

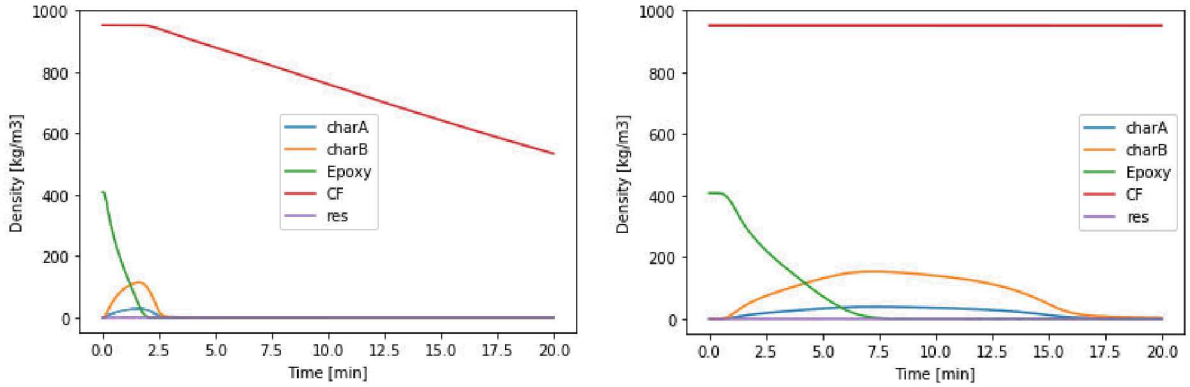

(a) (b)

Figure 5. Depletion of solid phase species for the simulation for the ceramic back faces for (a) 80kW flux and (b) 30kW flux

The species density curves along with the TGA results in Figure 2 indicate that only the ceramic 80kW and 70kW sample simulations are getting hot enough to replicate the experimental results. Since flaming ignition was seen in the experiments, but not modeled in the simulation, an additional heat flux was added to the top surface of the composite. A far field radiative source with temperatures ranging from 1526C to 126C (1800K to 400K) was examined. The 526C (800K) source, on average, had best agreement for all the heat fluxes for both the backing materials. To try to echo the effect of the flame, the heat source was only on if two conditions were met: the temperature was above 325 C (the ignition temperature [10]) and the density of epoxy was greater than zero (which assumes that the epoxy is generating the fuel for the flame). Figure 6 shows the new mass loss results for both backing materials.

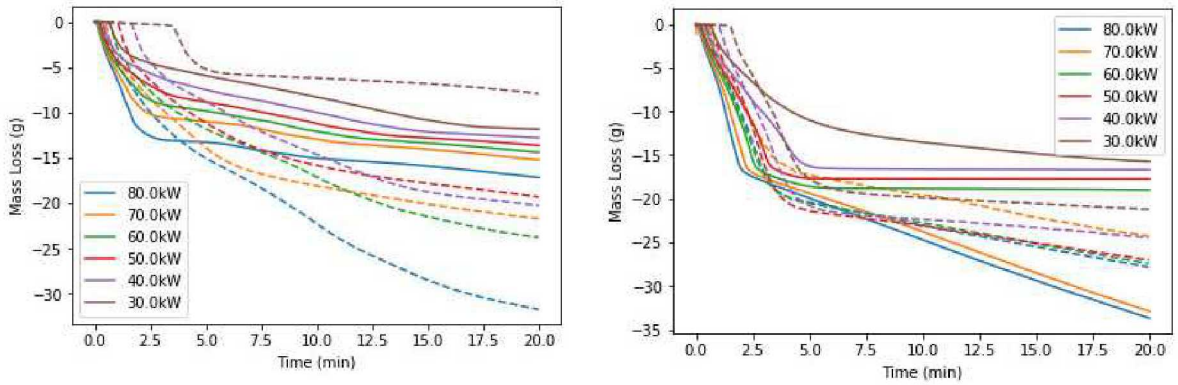

(a) (b)

Figure 6. Comparison of simulations (solid) with additional heat flux to account for flaming ignition to experiments (dashed) for heat fluxes from 30kW to 80kW for (a) the aluminum back face and (b) the ceramic back face

In general, the agreement between experiment and simulation improved, particularly for the ceramic backing. However, the total mass loss is still low for the aluminum backing. The change in density plots (Figure 7 and Figure 8) show that while the epoxy and char are being consumed faster, the carbon fiber is (relatively) unaffected.

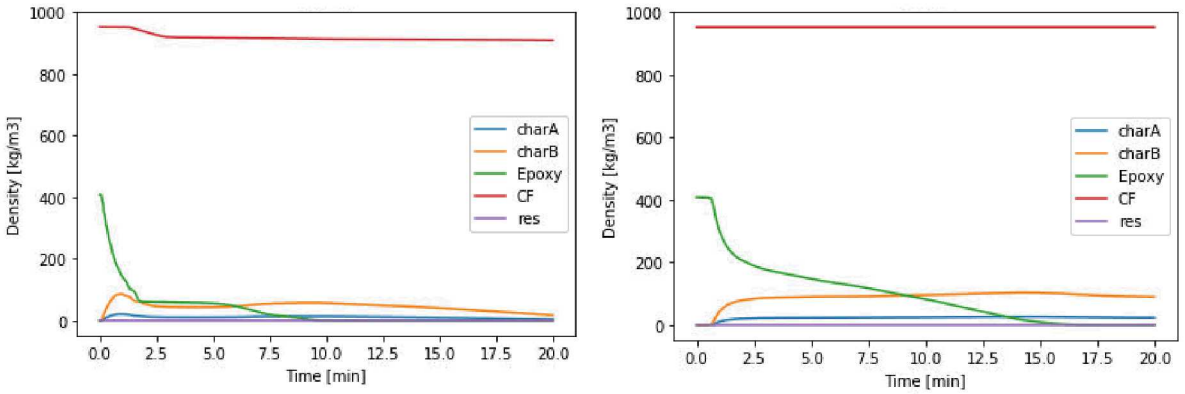

(a) (b)

Figure 7. Depletion of solid phase species for the simulation with additional heat flux to account for flaming ignition for the aluminum back faces for (a) 80kW flux and (b) 30kW flux

Examining the temperature profiles for the samples, the issue lies with the poor agreement between the mechanism and the TGA data for the 600C to 700C range. The samples that stay below or above this range have much better agreement, particularly with respect to total mass loss. This indicates that in order to achieve better agreement, a modification to the simplified mechanism is needed – perhaps an additional reaction that is activated in this temperature range. However, as Bal and Rein have shown, additional steps increase uncertainty [17].

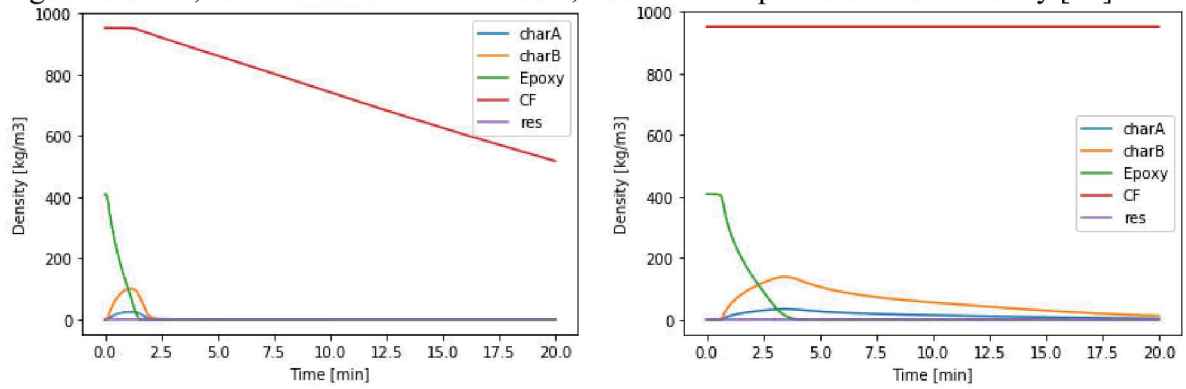

(a) (b)

Figure 8. Depletion of solid phase species for the simulation with additional heat flux to account for flaming ignition for the ceramic back faces for (a) 80kW flux and (b) 30kW flux

Summary and Future Work

A computational model of decomposing carbon fiber epoxy composite was compared to experimental results for two backing materials and a range of heat fluxes. Initially, results were qualitatively similar, though the simulation underpredicted the mass loss. Adding an additional heat flux as a surrogate for heat generated by a flame improved agreement. The best agreement was seen for samples that didn't reside in the 700C to 800C temperature range for long periods of time, as that is where the simplified mechanism has the poorest agreement with the TGA data.

Future work includes explicitly modeling the gas phase flame by coupling Sierra Thermal/Fluids: Fuego (low mach number CFD with combustion models) to Sierra Thermal/Fluids: Aria (multiphysics FEM). Additionally, adding an additional reaction in the 600C to 700C range or adjustments to the existing reaction could improve mass agreement. Additional, a sensitivity study of the material properties and boundary conditions will give further insight into the uncertainty associated with input parameters.

Acknowledgments
Sandia National Laboratories is a multimission laboratory managed and operated by National Technology and Engineering Solutions of Sandia, LLC., a wholly owned subsidiary of Honeywell International, Inc., for the U.S. Department of Energy National Nuclear Security Administration under contract DE-NA0003525.

References

[1] J. G. Quintiere, R. N. Walters, and S. Crowley, "Flammability Properties of Aircraft Carbon-Fiber Structural Composite," 2007.

[2] A. B. Dodd, B. Shelden, and K. L. Erickson, "Numerical Simulation of Decomposition and Combustion of an Epoxy-Carbon-Fiber Composite," in *Interflam*, 2011.

[3] M. B. McKinnon, Y. Ding, S. I. Stoliarov, S. Crowley, and R. E. Lyon, "Pyrolysis model for a carbon fiber/epoxy structural aerospace composite," *J. Fire Sci.*, vol. 35, no. 1, pp. 36–61, 2017.

[4] Y. Bai and T. Keller, "Time dependence of material properties of frp composites in fire," *J. Compos. Mater.*, vol. 43, no. 21, pp. 2469–2484, 2009.

[5] J. Zhang, M. A. Delichatsios, T. Fateh, M. Suzanne, and S. Ukleja, "Characterization of flammability and fire resistance of carbon fibre reinforced thermoset and thermoplastic composite materials," *J. Loss Prev. Process Ind.*, vol. 50, pp. 275–282, Nov. 2017.

[6] H. L. N. Mcmanus and G. S. Springer, "High Temperature Thermomechanical Behavior of Carbon-Phenolic and Carbon-Carbon Composites, I. Analysis," *J. Compos. Mater.*, vol. 26, no. 2, pp. 206–229, 1992.

[7] A. P. Mouritz *et al.*, "Review of fire structural modelling of polymer composites," *Compos. Part A Appl. Sci. Manuf.*, vol. 40, no. 12, pp. 1800–1814, 2009.

[8] N. Grange, K. Chetehouna, N. Gascoin, A. Coppalle, I. Reynaud, and S. Senave, "One-dimensional pyrolysis of carbon based composite materials using FireFOAM," *Fire Saf. J.*, vol. 97, pp. 66–75, Apr. 2018.

[9] P. Krysl, W. T. Ramroth, L. K. Stewart, and R. J. Asaro, "Finite element modelling of fibre reinforced polymer sandwich panels exposed to heat," *Int. J. Numer. Methods Eng.*, vol. 61, no. 1, pp. 49–68, 2004.

[10] J. P. Hidalgo, R. Hadden, S. Welch, and P. Pironi, "Effect of Thickness on the Ignition Behavior of Carbon Fibre Composite Materials used in High Pressure Vessels," *Eighth Int. Semin. Fire Explos. Hazards*, pp. 353–363, 2016.

[11] J. P. Hidalgo, P. Pironi, R. M. Hadden, and S. Welch, "A framework for evaluating the thermal behaviour of carbon fibre composite materials," *Eur. Symp. Fire Saf. Sci.*, pp. 195–200, 2015.

[12] J. P. Hidalgo, R. Hadden, S. Welch, and P. Pironi, "Experimental Study of the Burning Behavior of a Commercial Carbon Fibre Composite Material used in High Pressure Vessels," *ECCM17 - 17th Eur. Conf. Compos. Mater.*, no. June, p. 8, 2016.

[13] P. K. Notz, S. R. Subia, M. M. Hopkins, H. K. Moffat, D. R. Noble, and T. O. Okusanya, "SIERRA Multimechanics Module: Aria User Manual," Albuquerque, NM, 2016.

[14] C. Lautenberger and C. Fernandez-Pello, "Generalized pyrolysis model for combustible solids," *Fire Saf. J.*, vol. 44, no. 6, pp. 819–839, 2009.

[15] American Society for Metals. Metals Handbook Committee, *ASM Handbook Volume 2: Properties and Selection: Nonferrous Alloys and Special-Purpose Materials*. 1990.

[16] F. Incropera and D. DeWitt, *Fundamentals of Heat and Mass Transfer*. New York: J. Wiley, 2002.

[17] N. Bal and G. Rein, “On the effect of inverse modelling and compensation effects in computational pyrolysis for fire scenarios,” *Fire Saf. J.*, vol. 72, pp. 68–76, 2015.